ACS APPLIED MATERIALS & INTERFACES

Research Article

www.acsami.org

Detecting Kallikrein Proteolytic Activity with Peptide-Quantum Dot Nanosensors

Joyce C. Breger,[†,§] Kim E. Sapsford,[∥] Jessica Ganek,[∥] Kimihiro Susumu,[‡,⊥] Michael H. Stewart,[‡] and Igor L. Medintz*[,†]

[†]Center for Bio/Molecular Science and Engineering, Code 6900, and [‡]Optical Sciences Division, Code 5600, U.S. Naval Research Laboratory, Washington, DC, 20375 United States

[§]American Society for Engineering Education, Washington, DC 20036 United States

[∥]OMPT/CDRH/OSEL/DB, U.S. Food and Drug Administration, Silver Spring, Maryland 20993 United States

[⊥]Sotera Defense Solutions, Inc., Columbia, Maryland 21046 United States

ABSTRACT: Contamination and adulterants in both naturally derived and synthetic drugs pose a serious threat to the worldwide medical community. Developing rapid and sensitive sensors/devices to detect these hazards is thus a continuing need. We describe a hydrophilic semiconductor quantum dot (QD)-peptide Förster resonance energy transfer (FRET) nanosensor for monitoring the activity of kallikrein, a key proteolytic enzyme functioning at the initiation of the blood clotting cascade. Kallikrein is also activated by the presence of an oversulfated contaminant recently found in preparations of the drug heparin. Quantitatively monitoring the activity of this enzyme within a nanosensor format has proven challenging because of inherent steric and kinetic considerations. Our sensor is designed around a central QD donor platform which displays controlled ratios of a modular peptidyl substrate. This peptide, in turn, sequentially expresses a terminal oligohistidine motif that mediates the rapid self-assembly of peptides to the QD surface, a linker-spacer sequence to extend the peptide away from the QD surface, a kallikrein recognized-cleavage site, and terminates in an acceptor dye-labeling site. Hydrophilic QDs prepared with compact, zwitterionic surface coatings were first evaluated for their ability to self-assemble the dye-labeled peptide substrates. An optimized two-step protocol was then utilized where high concentrations of peptide were initially digested with purified human kallikrein and samples collected at distinct time points were subsequently diluted into QD-containing solutions for assaying. This sensor provided a quantitative FRET-based readout for monitoring kallikrein activity and comparison to a calibration curve allowed estimation of the relevant Michaelis–Menten kinetic descriptors. The results further suggest that almost any protease should be amenable to a QD-based FRET assay format with appropriate design considerations.

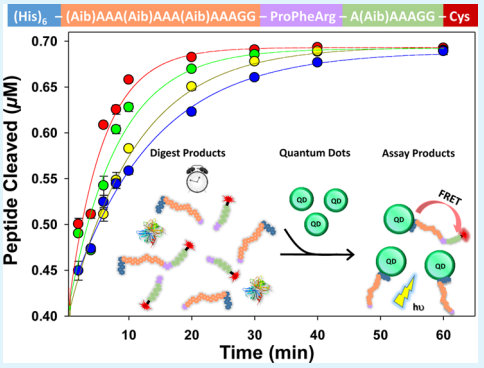

KEYWORDS: *fluorescence, nanoparticle, biosensor, quantum dot, FRET, enzyme, protease, kallikrein, substrate, K_m, nanocrystal, blood clotting, adulterant, assay*

1. INTRODUCTION

The advent of globalization has meant that most medicines and drug formulations are now sourced internationally creating greater possibilities of either unintentional contamination because of poor manufacturing quality control or even wholesale adulteration during preparation.[1−3] In an era of diminishing government resources, this will require development of robust cost-effective assays for testing drug purity.[4−6] The most prominent recent example of drug adulteration with widespread health impact was that of oversulfated chondroitin sulfate (OSCS) contamination in the world heparin supply.[7,8] Heparin, one of the most popular anticoagulant drugs for treating blood clotting issues, is a highly sulfated glycosaminoglycan consisting of sulfated disaccharide repeating units of iduronic acid/glucoronic acid and glucosoamine and is derived primarily from porcine intestinal mucosa.

Structurally similar to heparin, the presence of OSCS contamination has been shown to trigger aberrant activity of endogenous kallikrein in human plasma. OSCS and similar highly charged polyanionic polymers can alter several enzymatic cascades in plasma, affecting coagulation, fibrinolysis, inflammation, and vasculature function.[8] Silverberg et al., demonstrated the activation of the kinin-kallikrein pathway, which functions at the initiation of blood clotting, through the contact of factor XII with a negatively charged surface.[9] Highly sulfated polysaccharides like OSCS act as a negatively charged surface activating the contact system and the kinin-kallikrein pathway leading to hypotension as well as other adverse effects.[8] At the molecular level, kallikrein, which is a serine

Received: April 14, 2014
Accepted: June 23, 2014
Published: July 8, 2014

dx.doi.org/10.1021/am502135h | *ACS Appl. Mater. Interfaces* 2014, 6, 11529−11535

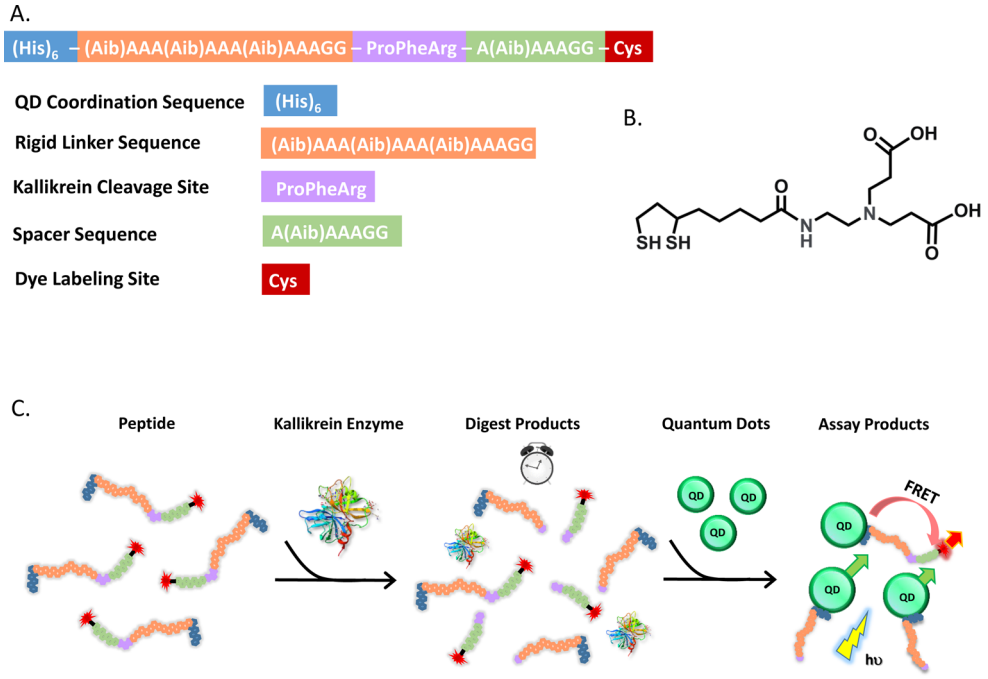

Figure 1. QD-FRET assay design elements. (A) Peptide sequence and summary overview highlighting the modular functional elements. (B) Chemical structure of the QD surface-functionalizing ligand. (C) Schematic illustrating QD-FRET based assay format for measuring kallikrein enzymatic activity. Peptide is digested with kallikrein and samples are removed at select time points. Samples are then added to QD and the resulting FRET monitored to extrapolate the proteolytic rate versus time by using a calibration curve.

protease, catalyze the excision of kinins such as kallidin and bradykinin from high molecular weight kininogen through preferential cleavage of Arg−Ser peptide bonds.[10] In turn, bradykinin functions by activating the intrinsic blood clotting cascade among a host of other roles. Therefore, monitoring the activity of endogenous kallikrein and especially its aberrant activation and upregulation has not only significant clinical implications but can also potentially signal the presence of OSCS. Here, we describe a quantum dot (QD) based nanosensor capable of quantitatively assaying kallikrein activity with a view toward utilizing it as an indicator for OSCS presence.

QDs offer several unique advantages over traditional organic fluorophores which make them attractive candidates for fluorescence-based chemo/biosensors.[11−13] QDs are characterized by high quantum yields (QY), exceptional photostability, and broad excitation spectra that are coupled to narrow size-tunable emission spectra.[11,12] Furthermore, the nontrivial QD surface area makes them particularly useful as biosensing platforms. Within this role, QDs typically provide two key properties - that of a central nanoscaffold around which the sensor is assembled and a central energy-harvesting donor which actively participates in Förster resonance energy transfer (FRET) or charge transfer based biosensing.[14−18] For proteolytic sensing in particular, the QDs are ratiometrically decorated with acceptor dye-labeled peptides or proteins by some linkage that also contains the necessary cleavage sequence. When implemented with the appropriate bioconjugation chemistry, the acceptor-fluorophores will tend to adopt a centrosymmetrical position around the QD donor.[15,16,19] Proteolysis cleaves the linkage, altering the QD-donor/dye acceptor proximity which, in turn, diminishes the FRET efficiency thus providing signal transduction.[15,19]

The simplicity inherent to this sensor design has led to development of QD-based FRET sensors targeting various different proteases including matrix metalloproteinases, collagenase, caspase 1, caspase 3, trypsin, thrombin, chymotrypsin, botulinum neurotoxin A, papain, proteinase K, urokinase-type plasminogen activator, etc.[15,19−25] However, not all proteases easily lend themselves to this sensor format owing to two underlying issues. The first is that of steric hindrance, where the physical size of larger proteases do not allow them to properly access, bind to and cleave substrates in the confines of the tight QD interface. This problem can be exacerbated when using QDs solubilized with large-high molecular weight poly(ethylene glycol) and related polymeric molecular surfaces.[26] Potential solutions to address this include appending a rigid linker onto the substrate to extend the recognition sequence away from the QD surface into a more available conformation or utilizing a two-step assay where QDs are added following substrate digestion by enzyme and essentially function as a visualization reagent.[21,22,25,27] The other complication is that of slower inherent specific activities coupled to K_m values in the higher micromolar to millimolar range. Given the standard fixed enzyme concentration/excess substrate assay format, this frequently means that the substrate (i.e., QD-assembly) becomes a limiting reagent since it cannot be reconstituted or function in the necessary excesses required. This can be somewhat overcome by using an excess enzyme or progress curve format but at the cost of requiring a significantly more complicated integrated analysis.[28] Here, we adapt the QD-FRET format to target the activity of kallikrein (Figure 1), a protease found at the apex of the blood clotting cascade and which provides challenges to this nanosensing format from both a steric and kinetic perspective. Our sensor is based on the aforementioned two-step assay[21,22,25] with QDs added following substrate digestion by the protease and demonstrates

the ability to quantitatively monitor enzyme activity along with determining relevant Michaelis–Menten kinetic descriptors.

2. EXPERIMENTAL METHODS

2.1. Materials. Reagent grade chemicals were used as received. Phosphate buffered saline (137 mM NaCl, 10 mM phosphate, 2.7 mM KCl, pH 7.4, PBS) and Corning 96-well black polystyrene nonbinding plates were obtained from Sigma-Aldrich (St. Louis, MO). Cy3-maleimide monoreactive dye was purchased from Amersham Biosciences (Piscataway, NJ). Purified kallikrein enzyme was purchased from American Diagnostica (Stamford, CT). Doubly distilled water (ddH_2O) was obtained from a Nanopure Diamond water purification system (Barnested Dubuque, IA).

2.2. Semiconductor Quantum Dots. CdSe/ZnS core/shell QDs with a photoluminescence (PL) maxima centered at 525 nm were synthesized as described.[29] The nanocrystals were made hydrophilic by exchanging the native hydrophobic ligands with dihydroplipoic acid (DHLA) appended compact ligand (CL4) as described.[30] QD absorption and emission spectra are presented in Figure 2.

2.3. Peptide Synthesis, Labeling, and Purification. Peptide substrate sequence $(His)_6$-$(Aib)A_3(Aib)A_3(Aib)A_3$GG-ProPheArg-A-$(Aib)A_3$GG-Cys (where Aib is the artificial residue α-methylalanine) was synthesized by Bio Synthesis Inc. (Lewisville, TX). A discussion of peptide design and intended function is provided in the results and also summarized in Figure 1A. Monovalent Cy3 labeling of the cysteine-thiol and purification/desalting of the peptide were as described.[21,31] Desalted peptide-Cy3 was characterized by UV–visible absorption spectroscopy (Cy3 absorbance 150 000 $M^{-1}cm^{-1}$ at 553 nm) before being aliquoted, dried down and stored in a desiccator at −20 °C until required.

2.4. Quantum Dot Calibration Curve and Proteolytic Assays. Fluorescent data from FRET titrations and enzymatic assays were collected on a Tecan Infinite M1000 Dual Monochromator Mulifunction Plate Reader (Tecan, Research Triangle Park, NC) from samples aliquoted into 96 well microtiter assay plates. A standard curve was constructed by self-assembling an increasing molar ratio of labeled peptide per QD. Cy3-labeled peptide was dissolved in DMSO (approximately 5% of the final volume) then ddH_2O such that the final concentration was 100 μM. Five picomoles of 525 nm emitting QD samples were mixed with Cy3-peptide at molar ratios of peptide to QD ranging from 0 to 20 in buffer consisting of 50 mM tris(hydroxymethyl)aminomethane (Tris) and 113 mM NaCl at pH 8. QD and peptide solutions were mixed and incubated for 30 min at room temperature before FRET analysis.

For enzymatic assays, Cy3-peptide at a final concentration range of 0, 6.3, 12.5, 25, and 50 μM was mixed with kallikrein enzyme (final concentration 500 nM) and Tris buffer on ice. The reaction mixture was then placed on a heat block at 37 °C and, at defined time points, 10 μL samples were transferred to a 96-well plate on dry ice to immediately quench the reaction. Following digestion, frozen aliquots were thawed, each time point was appropriately diluted and mixed with five picomoles of QD such as to theoretically maintain 12 peptides per QD. These solutions were incubated for 30 min at room temperature before fluorescent analysis.

2.5. Data Analysis. The QD donor-Cy3 acceptor dye spectral overlap integral J in units of cm^3 M^{-1} is calculated using[32]

$$J = \int_0^\infty J(\lambda)\,d\lambda = \int_0^\infty F_D(\lambda)\varepsilon_A(\lambda)\lambda^4\,d\lambda \quad (1)$$

where $F_D(\lambda)$ is the normalized fluorescence intensity of the donor (dimensionless), $\varepsilon_A(\lambda)$ is the extinction coefficient of the acceptor (cm^{-1} M^{-1}), and λ is the wavelength (cm). The Förster distance R_0, which corresponds to the donor–acceptor separation distance that yields 50% energy transfer efficiency, was determined using[33,34]

$$R_0 = \left(\frac{[9000 \times (\ln 10)] \times \kappa^2}{128\pi^5 n_D{}^4 N_A} Q_D J\right)^{1/6} \quad (2)$$

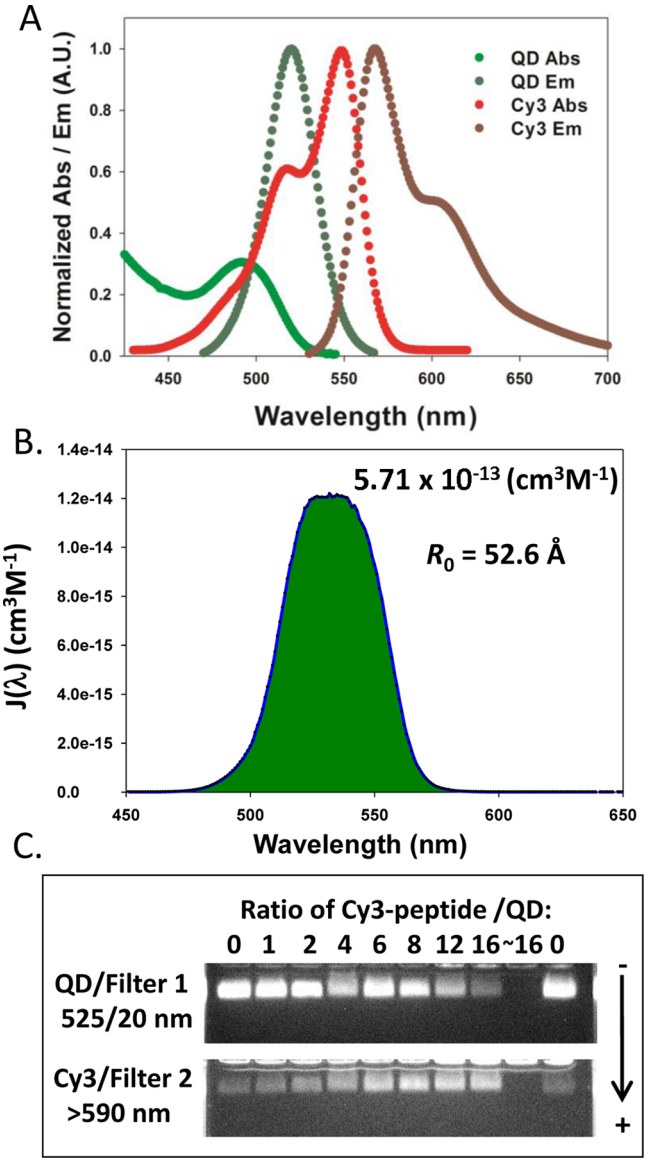

Figure 2. FRET parameters and peptide assembly to QD. (A) Normalized absorption/emission profiles of 525 nm QD (donor) and Cy3 (acceptor) and (B) the resulting spectral overlap. (C) Agarose gel electrophoresis separation of Cy3-labeled peptide-QD conjugates. Ratios of peptide per QD are indicated, the sample marked "~16" indicates the equivalent amount of acceptor-labeled peptide without QD present. Samples were run on a 1% agarose gel in 1× TBE buffer (89 mM Tris, 89 mM boric acid, 2 mM EDTA, pH 8.5) and images collected with the indicated filters using 365 nm excitation to isolate the QD and FRET-sensitized Cy3 PL components. Note that there is some QD cross-talk into the filter 2 channel but Cy3 emission increases are only seen when sensitized by the QD and also track with ratio displayed per QD. A slight mobility shift with increasing peptide ratio is also seen.

where κ^2 is the orientation factor, Q_D is the donor quantum yield, n_D is the refractive index of the medium, N_A is Avogadro's number, and J is the overlap integral. FRET efficiency E_n (n is the ratio or valence of dye acceptors per Q_D) was determined using

$$E_n = \frac{F_D - F_{DA}}{F_D} \quad (3)$$

where F_D and F_{DA} designate the integrated fluorescence intensities of donor alone or donor in the presence of acceptor(s), respectively.[33,34] Peak heights may also be used and yield similar results. A Poisson

distribution function, $p(k,n)$, was utilized to describe heterogeneity present in conjugate valence where FRET E is transformed as[35]

$$E(n) = \sum_{k=1}^{n} p(k, n)E(k) \text{ with } p(k, n) = \frac{e^{-n}n^{k}}{k!} \quad (4)$$

Here, n is the average acceptor-to-QD valence used during reagent mixing, and k is the exact number of peptide-dyes conjugated to the QD. This equation allows us to estimate any deviation in observed FRET E due to assembly heterogeneity. Changes in FRET E following enzymatic digestion were used to determine the number of Cy3-labeled peptides that remained intact (equivalent to undigested substrate) by comparison to a corrected FRET calibration curve assembled as described above.[36,37] These were converted into corresponding units of enzymatic activity and kinetic data analyzed utilizing a nonlinear regression Michaelis–Menten kinetic module in Sigma Plot on the basis of

$$v = \frac{V[S]}{dt} = \frac{V[S]}{K_m + [S]} = \frac{k_{cat}[E]_0[S]}{k_1^{-1}(k_{-1} + k_{cat}) + [S]} \quad (5)$$

where v is the rate of substrate turnover, K_m is the Michaelis constant, S is substrate, E is enzyme, t is time, V is the maximum velocity (maximum rate), k_{-1} is the on-rate, k_1^{-1} is the off-rate, and k_{cat} is the catalytic or turnover rate constant.

3. RESULTS

3.1. Peptide and Assay Design. The modular design of our peptide structure is shown in Figure 1A highlighting the different functionalities provided by each module. The C-terminal hexahistidine tag, $(His)_6$ in blue, allows the peptide substrate to self-assemble to the QD surface via metal affinity coordination interactions. Rapid and high affinity ($K_d \approx 1$ nM) self-assembly occurs between the imidazole side chain groups on the oligohistidine sequences and the Zn^{2+} rich surface of the CdSe/ZnS core/shell QDs, while also providing for control over peptide display ratio and peptide orientation in many cases.[14,21,38] This is followed by a rigid helix/spacer sequence that extends the remaining portion of the peptide and dye away from the QD surface (orange). This spacer is composed of $[Aib(Ala)_3]_3$, followed by glycine residues which "break" the helical motif.[20] Next is the cleavage site, shown in purple, composed of ProPheArg where kallikrein cleaves after the arginine residue. Another, shorter rigid helical spacer sequence (shown in green) is placed after the cleavage site to extend away the terminal dye and prevent the peptide from folding back on the recognition sequence. The N-terminal cysteine (shown in red) provides a unique thiol group for site-specific acceptor dye-modification of the peptide by maleimide chemistry.

Figure 1C presents a schematic of the assay ultimately implemented here. Initially, we anticipated assembling peptide substrate to QD and then directly exposing that to the enzyme. However, the bulk size of kallikrein (~86 kDa consisting of a 52 kDa heavy chain linked by disulfides to 33 or 36 kDa light chains) did not allow for "on-QD" proteolytic activity even when tested with different surface functionalizing ligands (data not shown). Moreover, even if we could utilize such an on-QD format, the amount of QD-substrate needed to access the conventional excess substrate format probably could not be easily realized given a limited QD supply. We thus implemented a modified two-step assay where a range of much higher peptide concentrations are digested by enzyme with discrete samples concurrently collected over time. These time-point samples are then appropriately diluted and added to the QDs in the final step. Only intact peptides can adhere to the QD surface and undergo FRET as the digested His_6-portion of the peptide is separated from the dye; measuring FRET efficiency here provides a direct window allowing us to follow enzyme activity.

3.2. Spectral Overlap and FRET Efficiency. For the central FRET donor, we utilize 525 nm emitting QDs (quantum yield ~20%) functionalized with a DHLA-based zwitterionic compact ligand (Figure 1B). These are among the smallest ligands available to functionalize QDs while still providing colloidal stability across a wide pH range.[30] The peptide substrate was labeled with a Cy3-acceptor dye yielding an overlap integral value of 5.71×10^{-13} cm^3 M^{-1} with a corresponding Förster distance or R_0 of 53 Å for this donor–acceptor pair. See Figure 2A, B for absorption/emission spectra and a plot of $J(\lambda)$, the spectral overlap integrand, versus wavelength.

Assembly of the peptide onto the QD was verified by monitoring mobility shifts with agarose gel electrophoresis (Figure 2C). As visualized in these figures with the use of appropriate filters, FRET can be confirmed on the gel by a steady decrease in QD donor PL along with an increase in sensitized Cy3 emission which tracks as a function of increasing acceptor ratio per QD. We also note that the peptide's increasing presence, that is, increasing mass, when assembled onto the QDs at increasing ratios and slight positive charge results in a slight decrease in mobility shift or migration in the gel. An increasing ratio of Cy3-labeled peptide substrate was then assembled onto the QDs and PL spectra collected. Figure 3A shows deconvoluted spectra highlighting QD donor quenching along with the concomitant Cy3-acceptor sensitization as a function of peptide valence. When QD samples were incubated with equivalent amounts of free Cy3 acceptor dye there was no significant FRET observed, confirming the specificity of peptide assembly to the QD (data not shown). Figure 3B plots the QD PL loss, acceptor sensitization, corresponding FRET efficiency E along with the correction to this for assembly heterogeneity. The high rate of FRET inherent to this system is clearly observed as the QD donor is ~80% quenched at an average display ratio of 4–5 peptides per QD and approaches 100% quenching between 15 and 20 peptides per QD. Analysis of this data places the acceptor dye at an average separation distance of ~60 Å from the QD donor core. The corresponding acceptor/donor ratio data, both experimental and corrected, is shown plotted out as a function of Cy3 ratio per QD in Figure 3C and this would subsequently serve as a calibration or standard curve for converting changes in FRET efficiency into units of activity. Use of such ratiometric data is preferred over just QD donor loss, or acceptor sensitization, as it is inherently less sensitive to intensity, concentration, and instrumental fluctuations.

3.3. Kallikrein Proteolytic Assay. For the assay, increasing concentrations of excess (>10×) Cy3-labeled kallikrein substrate peptide (0 and 6.3, 12.5, 25, and 50 μM) were digested in reactions against a fixed concentration of 500 nM enzyme at the physiological temperature of 37 °C. During the reaction course, 10 μL test samples were removed every 10 min and flash-frozen on dry ice to instantly quench activity. Following the reaction, these samples were then diluted into Tris buffer containing 5 picomoles of 525 nm QD, see Figure 4. Dilutions were meant to yield an average of 12 peptides per QD; as shown in Figure 3B this would access the widest, most dynamic range of QD PL loss and corresponding FRET E. The observed changes in acceptor/donor ratio (i.e., FRET E) were

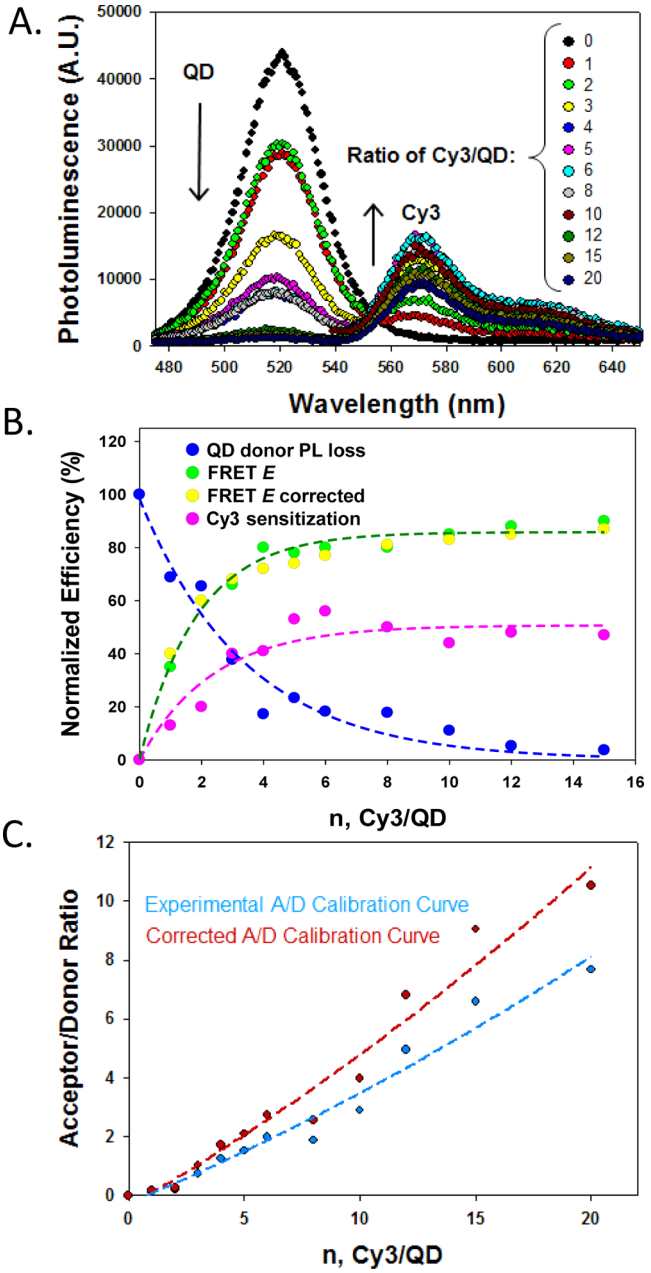

Figure 3. QD-to-Cy3-peptide FRET efficiency and calibration curve. (A) Deconvolved donor and acceptor PL spectra from assembling the indicated increasing number of Cy3-peptide per QD. (B) QD donor PL intensity loss at 525 nm (blue, units-right axis) plotted as a function of the number of Cy3-peptide per QD along with the Cy3 acceptor sensitization (pink) at 565 nm from data in (A).[22,23] Corresponding FRET *E* and corrected FRET *E* where determined from panel A in this representative example using the integrated area under each deconvolved curve and are plotted as a function of the number of Cy3-peptide/QD. Lines of best fit are added to highlight trends. (C) Experimental and corrected calibration curves. A = acceptor, D = donor.

then converted into concentration (μM) of peptide cleaved versus time, Figure 4.

Analyzing this data allows us to extract the initial proteolytic rates, see Figure 4-inset. Fitting these using a nonlinear regression in the Michaelis–Menten module provided by Sigma Plot yields a maximum velocity V of 0.028 ± 0.005 μM/min and estimates a K_m of 4.4 ± 0.1 μM, a k_{cat} of 9.3 ± 0.3 × 10^{-4} s^{-1} and an estimated k_{cat}/K_m of 2 × 10^{-4} μM^{-1} s^{-1}; the latter is a second-order rate constant commonly used to characterize enzyme efficiency. As expected, the highest initial rate is seen for the highest substrate concentration used. For comparison a K_m of 11 μM, a k_{cat} of 3.45 s^{-1} and a k_{cat}/K_m of 0.31 μM^{-1} s^{-1} was previously reported by Mikolajczyk for prostate-specific human kallikrein.[39] We ascribe some of the variation between these sets of values to use of different enzyme sources and assay formats. For example, the latter comparison enzyme mentioned is not specific to nor identical to that found in the blood clotting cascade.

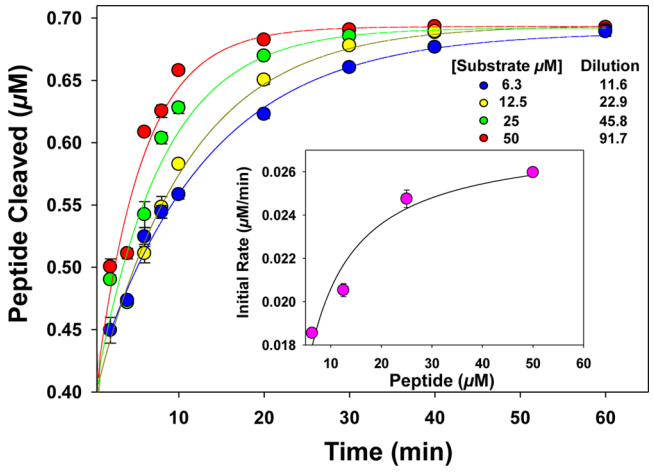

Figure 4. Kinetic assay data. Kallikrein digestion of Cy3-labeled peptide substrate as a function of time at the indicated peptide substrate concentrations. Inset plots the initial rates versus substrate concentration and utilizes a nonlinear regression fitting based on the Michaelis–Menten kinetic model. The latter were used to estimate V_{max}, K_m, and k_{cat}. Dilutions utilized with each sample are shown.

4. DISCUSSION AND CONCLUSIONS

Here we present a proof of concept showing that QD-FRET based nanosensors can indeed be applied to monitoring the activity of challenging proteases. Kallikrein inherently provides two major issues for such a sensing format. The first is that the large enzyme size precludes an "on-QD" assay, which is something encountered before and previously addressed with a modified "2-step" assay.[21,25] Even if this protease were amenable to the on-QD format, the much higher K_m coupled with a somewhat lower k_{cat} (in comparison to high activity proteases such as trypsin or the caspases)[20,22,23] would not easily allow for a standard excess substrate assay format (substrate = QD-peptide conjugate) because of limits on the amount of accessible QD concentrations. Although this may seem like a disadvantage, such a format may actually better reflect native enzyme–substrate interactions as a growing body of research suggests that enzymatic activity may be enhanced at a nanoparticle interface for reasons that are still not fully understood.[28,36,40]

The complexity of how kallikrein is activated by OSCS and how this, in turn, impacts homeostasis in a patient make it hard to provide absolute values in terms of limits of detection (LOD) in general. The seminal work of Kishimoto showed a direct link between kallikreins upregulation and OSCS contamination in direct comparison to "pristine" Heparin which did not evoke a response.[41] This work also showed that OSCS can cause a ~6-fold increase in activity above the basal rate while activating the contact system. Bairstow showed a "no

observed effect level" for ≤3% OSCS contamination of Heparin in a pig model system suggesting that anything above this level may be of concern.[42] Thus, assaying for just the presence of OSCS is not sufficient as more information is needed including specifically if kallikrein has been activated. It is important to note that each patient will also manifest a slightly different basal rate of activity, activation and physiological response.

There may also be other direct benefits to using a QD-based assay format over that of direct monitoring of a fluorescent or FRET-peptide substrate. Kallikrein's native environment is that of plasma and blood with the presence of large amounts of proteins which invariably precludes fluorescent monitoring *in situ*. However, the ability of QD-FRET to be realized in a time-gated detection modality or with multiphoton excitation can allow for direct monitoring in such environments.[36,43−45] This ability would even allow for direct plasma kallikrein activation studies with known activators such as kaolin or dextran sulfate, OSCS and other structurally similar compounds, suggesting that potential contaminants or therapeutics against activation could also undergo extensive screening in the same format. Alternatively, this assay could be incorporated into a field-deployable microfabricated device where it could aid in monitoring blood products or therapeutics for similar contaminants. Lastly, and perhaps most importantly, these results suggest that many of the >500 putative proteases present in the human genome should be amenable to assaying with QD-FRET based platforms where the QD-substrate peptides are assembled using a similar modular design.[15,16,19]

AUTHOR INFORMATION

Corresponding Author

*E-mail: igor.medintz@nrl.navy.mil.

Notes

The authors declare no competing financial interest.

ACKNOWLEDGMENTS

Financial support is gratefully acknowledged from the NRL-NSI, ONR, and DTRA. K.E.S would like to thank Office of the Chief Scientist and Division of Biology FDA for financial support. Postdoctoral fellowship for J.C.B. administered by the American Society for Engineering Education (ASEE).

REFERENCES

(1) Liu, J. L.; Wong, M. H. Pharmaceuticals and Personal Care Products (PPCPs): A Review on Environmental Contamination in China. *Env. Int.* **2013**, *59*, 208−224.

(2) Posadzki, P.; Watson, L.; Ernst, E. Contamination and Adulteration of Herbal Medicinal Products (HMPs): An Overview of Systematic Reviews. *Eur. J. Clin. Pharm.* **2013**, *69*, 295−307.

(3) Almuzaini, T.; Sammons, H.; Choonara, I. Substandard and Falsified Medicines in the UK: A Retrospective Review of Drug Alerts (2001−2011). *BMJ Open* **2013**, *3*.

(4) Narsaiah, K.; Jha, S. N.; Bhardwaj, R.; Sharma, R.; Kumar, R. Optical Biosensors for Food Quality and Safety Assurance A Review. *J. Food Sci. Technol.* **2012**, *49*, 383−406.

(5) Gunar, O. V. Aspects of Investigating Microflora Contamination of Drugs (A Review). *Pharm. Chem. J.* **2011**, *45*, 93−102.

(6) Petroczi, A.; Taylor, G.; Naughton, D. P. Mission Impossible? Regulatory and Enforcement Issues to Ensure Safety of Dietary Supplements. *Food Chem. Toxicol.* **2011**, *49*, 393−402.

(7) Guerrini, M.; Beccati, D.; Shriver, Z.; Naggi, A.; Viswanathan, K.; Bisio, A.; Capila, I.; Lansing, J. C.; Guglieri, S.; Fraser, B.; Al-Hakim, A.; Gunay, N. S.; Zhang, Z.; Robinson, L.; Buhse, L.; Nasr, M.; Woodcock, J.; Langer, R.; Venkataraman, G.; Linhardt, R. J.; Casu, B.; Torri, G.; Sasisekharan, R. Oversulfated Chondroitin Sulfate is a Contaminant in Heparin Associated with Adverse Clinical Events. *Nat. Biotechnol.* **2008**, *26*, 669−675.

(8) Kishimoto, T. K.; Viswanathan, K.; Ganguly, T.; Elankumaran, S.; Smith, S.; Pelzer, K.; Lansing, J. C.; Sriranganathan, N.; Zhao, G.; Galcheva-Gargova, Z.; Al-Hakim, A.; Bailey, G. S.; Fraser, B.; Roy, S.; Rogers-Cotrone, T.; Buhse, L.; Whary, M.; Fox, J.; Nasr, M.; Dal Pan, G. J.; Shriver, Z.; Langer, R. S.; Venkataraman, G.; Austen, K. F.; Woodcock, J.; Sasisekharan, R. Contaminated Heparin Associated with Adverse Clinical Events and Activation of the Contact System. *New Eng. J. Med.* **2008**, *358*, 2457−2467.

(9) Silverberg, M.; Diehl, S. V. The Autoactivation of Factor-XII (Hageman-Factor) Induced by Low-MR Heparin and Dextran Sulfate—The Effect of the Activating Polyanion. *Biochem. J.* **1987**, *248*, 715−720.

(10) Levison, P. R.; Tomalin, G. The Kinetics of Hydrolysis of Some Extended N-Aminoacyl-L-Arginine Methyl Esters by Human-Plasma Kallikrein—Evidence for Substites S2 and S3. *Biochem. J.* **1982**, *203*, 149−153.

(11) Petryayeva, E.; Algar, W. R.; Medintz, I. L. Quantum Dots in Bioanalysis: A Review of Applications Across Various Platforms for Fluorescence Spectroscopy and Imaging. *Appl. Spectrosc.* **2013**, *67*, 215−252.

(12) Rosenthal, S. J.; Chang, J. C.; Kovtun, O.; McBride, J. R.; Tomlinson, I. D. Biocompatible Quantum Dots for Biological Applications. *Chem. Biol.* **2011**, *18*, 10−24.

(13) Tyrakowski, C. M.; Snee, P. T. A Primer on the Synthesis, Water-Solubilization, and Functionalization of Quantum Dots, Their Use as Biological Sensing Agents, and Present Status. *Phys. Chem. Chem. Phys.* **2014**, *16*, 837−855.

(14) Blanco-Canosa, J.; Wu, M.; Susumu, K.; Petryayeva, E.; Jennings, T. L.; Dawson, P. E.; Algar, W. R.; Medintz, I. L. Recent Progress in the Bioconjugation of Quantum Dots. *Coord. Chem. Rev.* **2014**, *263−264*, 101−137.

(15) Algar, W. R.; Kim, H.; Medintz, I. L.; Hildebrandt, N. Emerging Non-Traditional Förster Resonance Energy Transfer Configurations with Semiconductor Quantum Dots: Investigations and Applications. *Coord. Chem. Rev.* **2014**, *263−264*, 65−85.

(16) Kethineedi, V. R.; Crivat, G.; Tarr, M. A.; Rosenzweig, Z. Quantum Dot-NBD-Liposome Luminescent Probes for Monitoring Phospholipase A(2) Activity. *Anal. Bioanal. Chem.* **2013**, *405*, 9729−9737.

(17) Medintz, I. L.; Farrell, D.; Susumu, K.; Trammell, S. A.; Deschamps, J. R.; Brunel, F. M.; Dawson, P. E.; Mattoussi, H. M. Multiplex Charge Transfer Interactions Between Quantum Dots and Peptide-Bridged Ruthenium Complexes. *Anal. Chem.* **2009**, *81*, 4831−4839.

(18) Medintz, I. L.; Stewart, M. H.; Trammell, S. A.; Susumu, K.; Delehanty, J. B.; Mei, B. C.; Melinger, J. S.; Blanco-Canosa, J. B.; Dawson, P. E.; Mattoussi, H. Quantum-Dot/Dopamine Bioconjugates Function as Redox Coupled Assemblies for In Vitro and Intracellular pH Sensing. *Nat. Mater.* **2010**, *9*, 676−684.

(19) Kim, G. B.; Kim, Y. P. Analysis of Protease Activity Using Quantum Dots and Resonance Energy Transfer. *Theranostics* **2012**, *2*, 127−138.

(20) Medintz, I. L.; Clapp, A. R.; Brunel, F. M.; Tiefenbrunn, T.; Uyeda, H. T.; Chang, E. L.; Deschamps, J. R.; Dawson, P. E.; Mattoussi, H. Proteolytic Activity Monitored by Fluorescence Resonance Energy Transfer Through Quantum-Dot-Peptide Conjugates. *Nat. Mater.* **2006**, *5*, 581−589.

(21) Sapsford, K. E.; Granek, J.; Deschamps, J. R.; Boeneman, K.; Blanco-Canosa, J. B.; Dawson, P. E.; Susumu, K.; Stewart, M. H.; Medintz, I. L. Monitoring Botulinum Neurotoxin A Activity with Peptide-Functionalized Quantum Dot Resonance Energy Transfer Sensors. *ACS Nano* **2011**, *5*, 2687−2699.

(22) Boeneman, K.; Mei, B.; Dennis, A.; Bao, G.; Deschamps, J. R.; Mattoussi, H.; Medintz, I. L. Sensing Caspase 3 Activity with Quantum Dot-Fluorescent Protein Assemblies. *J. Am. Chem. Soc.* **2009**, *131*, 3828−3829.

(23) Prasuhn, D. E.; Feltz, A.; Blanco-Canosa, J. B.; Susumu, K.; Stewart, M. H.; Mei, B. C.; Yakovlev, A. V.; Loukov, C.; Mallet, J. M.; Oheim, M.; Dawson, P. E.; Medintz, I. L. Quantum Dot Peptide Biosensors for Monitoring Caspase 3 Proteolysis and Calcium Ions. *ACS Nano* **2010**, *4*, 5487−5497.
(24) Shi, L.; De Paoli, V.; Rosenzweig, N.; Rosenzweig, Z. Synthesis and Application of Quantum Dots FRET-Based Protease Sensors. *J. Am. Chem. Soc.* **2006**, *128*, 10378−10379.
(25) Lowe, S. B.; Dick, J. A. G.; Cohen, B. E.; Stevens, M. M. Multiplex Sensing of Protease and Kinase Enzyme Activity via Orthogonal Coupling of Quantum Dot−Peptide Conjugates. *ACS Nano* **2012**, *6*, 851−857.
(26) Dennis, A. M.; Sotto, D. C.; Mei, B. C.; Medintz, I. L.; Mattoussi, H.; Bao, G. Surface Ligand Effects on Metal-Affinity Coordination to Quantum Dots: Implications for Nanoprobe Self-Assembly. *Bioconjugate Chem.* **2010**, *21*, 1160−1170.
(27) Gemmill, K. B.; Deschamps, J. R.; Delehanty, J. B.; Susumu, K.; Stewart, M. H.; Glaven, R. H.; Anderson, G. P.; Goldman, E. R.; Huston, A. L.; Medintz, I. L. Optimizing Protein Coordination to Quantum Dots with Designer Peptidyl Linkers. *Bioconjugate Chem.* **2013**, *24*, 269−281.
(28) Algar, W. R.; Malonoski, A.; Deschamps, J. R.; Banco-Canosa, J. B.; Susumu, K.; Stewart, M. H.; Johnson, B. J.; Dawson, P. E.; Medintz, I. L. Proteolytic Activity at Quantum Dot-Conjugates: Kinetic Analysis Reveals Enhanced Enzyme Activity and Localized Interfacial "Hopping". *Nano Lett.* **2012**, *12*, 3793−3802.
(29) Snee, P. T.; Chan, Y.; Nocera, D. G.; Bawendi, M. G. Whispering Gallery Mode Lasing from a Semiconductor Nanocrystal/Microsphere Resonator Composite. *Adv. Mater.* **2005**, *17*, 1131−1136.
(30) Susumu, K.; Oh, E.; Delehanty, J. B.; Blanco-Canosa, J. B.; Johnson, B. J.; Jain, V.; Hervey, W. J.; Algar, W. R.; Boeneman, K.; Dawson, P. E.; Medintz, I. L. Multifunctional Compact Zwitterionic Ligands for Preparing Robust Biocompatible Semiconductor Quantum Dots and Gold Nanoparticles. *J. Am. Chem. Soc.* **2011**, *133*, 9480−9496.
(31) Sapsford, K. E.; Farrell, D.; Sun, S.; Rasooly, A.; Mattoussi, H.; Medintz, I. L. Monitoring of Enzymatic Proteolysis on a Electroluminescent-CCD Microchip Platform using Quantum Dot-Peptide Substrates. *Sens. Actuators, B* **2009**, *139*, 13−21.
(32) Stewart, M. H.; Huston, A.; Scott, A.; Oh, E.; Algar, W. R.; Deschamps, J.; Susumu, K.; Jain, V.; Prasuhn, D.; Blanco-Canosa, J.; Dawson, P.; Medintz, I. L. Competition Between FRET and Electron Transfer in Stoichiometrically-Assembled Quantum Dot-Fullerene Conjugates. *ACS Nano* **2013**, *7*, 9489−9505.
(33) Clapp, A. R.; Medintz, I. L.; Mauro, J. M.; Fisher, B. R.; Bawendi, M. G.; Mattoussi, H. Fluorescence Resonance Energy Transfer Between Quantum Dot Donors and Dye-Labeled Protein Acceptors. *J. Am. Chem. Soc.* **2004**, *126*, 301−310.
(34) Lakowicz, J. R. *Principles of Fluorescence Spectroscopy*, 3rd ed.; Springer: New York, 2006.
(35) Pons, T.; Medintz, I. L.; Wang, X.; English, D. S.; Mattoussi, H. Solution-Phase Single Quantum Dot Fluorescence Resonance Energy Transfer. *J. Am. Chem. Soc.* **2006**, *128*, 15324−15331.
(36) Medintz, I. L.; Uyeda, H. T.; Goldman, E. R.; Mattoussi, H. Quantum Dot Bioconjugates for Imaging, Labelling and Sensing. *Nat. Mater.* **2005**, *4*, 435−446.
(37) Algar, W. R.; Malanoski, A. P.; Susumu, K.; Stewart, M. H.; Hildebrandt, N.; Medintz, I. L. Multiplexed Tracking of Protease Activity Using a Single Color of Quantum Dot Vector and a Time-Gated Forster Resonance Energy Transfer Relay. *Anal. Chem.* **2012**, *84*, 10136−10146.
(38) Sapsford, K. E.; Pons, T.; Medintz, I. L.; Higashiya, S.; Brunel, F. M.; Dawson, P. E.; Mattoussi, H. Kinetics of Metal-Affinity Driven Self-Assembly Between Proteins or Peptides and CdSe-ZnS Quantum Dots. *J. Phys. Chem. C* **2007**, *111*, 11528−11538.
(39) Mikolajczyk, S. D.; Millar, L. S.; Marker, K. M.; Grauer, L. S.; Goel, A.; Cass, M. M. J.; Kumar, A.; Saedi, M. S. Ala217 is Important for the Catalytic Function and Autoactivation of Prostate-Specific Human Kallikrein 2. *Eur. J. Biochem.* **1997**, *246*, 440−446.
(40) Johnson, B. J.; Algar, W. R.; Malanoski, A. P.; Ancona, M. G.; Medintz, I. L. Understanding Enzymatic Acceleration at Nanoparticle Interfaces: Approaches and Challenges. *Nano Today* **2014**, *9*, 102−131.
(41) Kishimoto, T. K.; Viswanathan, K.; Ganguly, T.; Elankumaran, S.; Smith, S.; Pelzer, K.; Lansing, J. C.; Sriranganathan, N.; Zhao, G. L.; Galcheva-Gargova, Z.; et al. Contaminated Heparin Associated with Adverse Clinical Events and Activation of the Contact System. *New Eng. J. Med.* **2008**, *358*, 2457−2467.
(42) Bairstow, S.; McKee, J.; Nordhaus, M.; Johnson, R. Identification of a Simple and Sensitive Microplate Method for the Detection of Oversulfated Chondroitin Sulfate in Heparin Products. *Anal. Biochem.* **2009**, *388*, 317−321.
(43) Morgner, F.; Stufler, S.; Geißler, D.; Medintz, I. L.; Algar, W. R.; Susumu, K.; Stewart, M. H.; Blanco-Canosa, J. B.; Dawson, P. E.; Hildebrandt, N. Terbium to Quantum Dot FRET Bioconjugates for Clinical Diagnostics: Influence of Human Plasma on Optical and Assembly Properties. *Sensors* **2011**, *11*, 9667−9684.
(44) Clapp, A. R.; Pons, T.; Medintz, I. L.; Delehanty, J. B.; Melinger, J. S.; Tiefenbrunn, T.; Dawson, P. E.; Fisher, B. R.; O'Rourke, B.; Mattoussi, H. Two-Photon Excitation of Quantum Dot-Based Fluorescence Resonance Energy Transfer and its Applications. *Adv. Mater.* **2007**, *19*, 1921−1926.
(45) Algar, W. R.; Wegner, D.; Huston, A. L.; Blanco-Canosa, J. B.; Stewart, M. H.; Armstrong, A.; Dawson, P. E.; Hildebrandt, N.; Medintz, I. L. Quantum Dots as Simultaneous Acceptors and Donors in Time-Gated Forster Resonance Energy Transfer Relays: Characterization and Biosensing. *J. Am. Chem. Soc.* **2012**, *134*, 1876−1891.